Mutations of *POLR3A* Encoding a Catalytic Subunit of RNA Polymerase Pol III Cause a Recessive Hypomyelinating Leukodystrophy

Geneviève Bernard,[1,3] Eliane Chouery,[2] Maria Lisa Putorti,[3] Martine Tétreault,[3] Asako Takanohashi,[4] Giovanni Carosso,[4] Isabelle Clément,[3] Odile Boespflug-Tanguy,[5,6,7,8] Diana Rodriguez,[8,9,10] Valérie Delague,[11] Joelle Abou Ghoch,[2] Nadine Jalkh,[2] Imen Dorboz,[7,8] Sebastien Fribourg,[12] Martin Teichmann,[12] André Megarbane,[2,13] Raphael Schiffmann,[14] Adeline Vanderver,[4] and Bernard Brais[3,*]

Leukodystrophies are a heterogeneous group of inherited neurodegenerative disorders characterized by abnormal white matter visible by brain imaging. It is estimated that at least 30% to 40% of individuals remain without a precise diagnosis despite extensive investigations. We mapped tremor-ataxia with central hypomyelination (TACH) to 10q22.3-23.1 in French-Canadian families and sequenced candidate genes within this interval. Two missense and one insertion mutations in five individuals with TACH were uncovered in *POLR3A*, which codes for the largest subunit of RNA polymerase III (Pol III). Because these families were mapped to the same locus as leukodystrophy with oligodontia (LO) and presented clinical and radiological overlap with individuals with hypomyelination, hypodontia and hypogonadotropic hypogonadism (4H) syndrome, we sequenced this gene in nine individuals with 4H and eight with LO. In total, 14 recessive mutations were found in 19 individuals with TACH, 4H, or LO, establishing that these leukodystrophies are allelic. No individual was found to carry two nonsense mutations. Immunoblots on 4H fibroblasts and on the autopsied brain of an individual diagnosed with 4H documented a significant decrease in POLR3A levels, and there was a more significant decrease in the cerebral white matter compared to that in the cortex. Pol III has a wide set of target RNA transcripts, including all nuclear-coded tRNA. We hypothesize that the decrease in POLR3A leads to dysregulation of the expression of certain Pol III targets and thereby perturbs cytoplasmic protein synthesis. This type of broad alteration in protein synthesis is predicted to occur in other leukoencephalopathies such as hypomyelinating leukodystrophy-3, caused by mutations in aminoacyl-tRNA synthetase complex-interacting multifunctional protein 1 (*AIMP1*).

Leukodystrophies are a heterogeneous group of inherited neurodegenerative disorders characterized by abnormal central-nervous-system white matter.[1] It is estimated that at least 30% to 40% of individuals still remain without a precise diagnosis despite extensive investigations.[2] We recently described tremor-ataxia with central hypomyelination (TACH), a form of childhood-onset hypomyelinating leukodystrophy with prominent tremor and cerebellar signs and mapped its locus to 10q22.3-q23.31.[3] Another hypomyelinating leukodystrophy, leukodystrophy with oligodontia (LO) (MIM 607694), was also mapped to 10q22 in a Syrian family.[4,5] Both TACH and LO have clinical and radiological overlap with another unmapped form of hypomyelinating leukodystrophy referred to as hypomyelination with hypodontia and hypogonadotropic hypogonadism (4H) syndrome (MIM 612440).[6–9] In this study, we report that the three conditions are allelic and caused by recessive mutations in *POLR3A* (MIM 610210) encoding the largest subunit of human RNA polymerase III (Pol III).

This project was approved by the institutional ethics committee of the Centre de Recherche du Centre hospitalier de l'Université de Montréal (CRCHUM), Montreal, Canada; the Unité de Génétique Médicale, Saint-Joseph University, Riad El Solh, Lebanon; the Comité de Protection des Personnes Sud-Est VI, Centre Hospitalier Universitaire, Clermont-Ferrand, France; the institutional review board of the National Institute of Neurological Disorders and Stroke, National Institute of Health, Bethesda, MA, USA; and the Children's National Medical Center, Washington D.C., USA. Informed consent was obtained from all participants. By combining the published TACH interval,[3] the mapping of a predicted historical recombinant in a new French-Canadian TACH family,[10] and the published candidate interval of LO,[5] we narrowed the candidate interval to a 2.99 Mb region on 10q22.3

[1]Departments of Pediatrics, Neurology and Neurosurgery, Division of Pediatric Neurology, Montreal Children's Hospital, McGill University Heath Center, Montreal, Quebec H3H 1P3, Canada; [2]Unité de Génétique Médicale et laboratoire associé, INSERM à l'unité UMR_S 910, Faculté de Médecine, Université Saint-Joseph, Beirut, 11-5076 Riad El Solh, Lebanon; [3]Neurogenetics of Motion Laboratory, Montreal Neurological Institute, McGill University, Montreal, Quebec H3A 2B4, Canada; [4]Neurology Department, Children's National Medical Center, Washington, D.C. 20010, USA; [5]Assistance Publique des Hôpitaux de Paris (APHP), Reference Center for Leukodystrophies, Hôpital Robert Debré, Paris 75019, France; [6]Université Paris Diderot, Sorbonne Paris Cité, 75205 Paris Cedex 13, France; [7]Institut National de la Santé et de la Recherche Médicale (INSERM) U931, 63001 Clermont Ferrand, France; [8]INSERM U676, 75935 Paris Cedex 19, France; [9]AP-HP, Hôpital Armand Trousseau, service de neurologie pédiatrique, 75571 Paris Cedex 12, France; [10]UPMC Université de Paris 06, 75252 Paris Cedex 05, France; [11]INSERM UMR_S 910, Génétique Médicale et Génomique Fonctionnelle, Faculté de Médecine de la Timone, Marseille 13385, France; [12]Institut Européen de Chimie et Biologie (I.E.C.B.), INSERM, Université de Bordeaux, Pessac 33607, France; [13]Institut Jérôme Lejeune, Paris 75015, France; [14]Institute of Metabolic Disease, Baylor Research Institute, Dallas, TX 75226, USA
*Correspondence: bernard.brais@mcgill.ca

(rs2116829-rs927452), containing approximately 15 genes. Considering the relatively small size of the interval and the fact that it includes ten promising candidate genes, we chose to sequence these genes rather than perform next-generation sequencing. Sequencing of the exons, exon-intron boundaries, and 3′ and 5′ untranslated regions (UTRs) of the following six genes did not uncover any mutation: eukaryotic translation initiation factor 5A-like 1 (*EIF5AL1*), potassium large conductance calcium-activated channel, subfamily M, alpha member 1 (*KCNMA1* [MIM 600150]), peptidylprolyl isomerase F precursor (*PPIF* [MIM 604486]), ribosomal protein S24 isoform b (*RPS24* [MIM 602412]), pulmonary surfactant-associated protein A1 (*SFTPA1* [MIM 178630]), pulmonary surfactant-associated protein A2 (*SFTPA2* [MIM 178642]). *POLR3A* was considered a candidate gene because it is responsible for tRNA and 5S transcription that, if perturbed, should have an impact on protein synthesis. Sequencing of the 31 exons, exon-intron boundaries, and 5′ and 3′ UTRs of *POLR3A* (NM_007055.3) uncovered a homozygous missense c.2015G>A (p.Gly672Glu) mutation in *POLR3A* in 3 out of 4 TACH families from the same region of Quebec: families II (individuals 2–4), III (individual 5), and IV (individual 6) (Table 1). Individuals 2 and 3 are brothers and their parents are consanguineous, whereas individual 4 is a deceased distant cousin. The parents of individual 5 are distantly related, whereas the parents of individual 6 are not known but are suspected to be related. The other individual with TACH (individual 1, family I) carries two different mutations: c.1674C>G (p.Phe558Leu) and c.3742insACC (p.1248insThr) (Table 1). Sequencing of *POLR3A* in individuals with LO uncovered the following mutations: c.2003+18G>A (p.Tyr637-CysfsX650) in the previously published consanguineous Syrian family[5] (family X, where individuals 12–15 are siblings and individuals 16–17 are their first-degree cousins), c.418C>T (p.Arg140X) and c.2554A>G (p.Met852Val) in the European individual, and c.2171G>A (p.Cys724Tyr) in the Guatemalan individual (Table 1). The clinical overlap between TACH, LO, and 4H led to the sequencing of nine individuals with 4H. Five individuals with 4H were compound heterozygotes for mutations in *POLR3A*, whereas in four clinically similar individuals with 4H, no mutations were uncovered. Individuals 7, 8, 9, and 10 were part of the original individuals with 4H described.[8] In total, 19 individuals belonging to 12 families were found to be homozygotes or compound heterozygotes for 14 different putative *POLR3A* mutations: eight missense, one three-base-pairs insertion, three nonsense, and two splice-site mutations (Table 1). Among them, nine mutations result in amino acid change or insertion in regions that are highly conserved across different species (Figure 1). None of the participants are homozygous for nonsense mutations. All parents were unaffected and found to carry one of their affected child's mutations, whereas unaffected siblings were never found to carry two mutations. All variants were absent in more than 250 French-Canadian, European, and Lebanese control chromosomes.

The locations of the different missense mutations are represented in Figure 1. Pol III's POLR3A (RPC1) and Pol lI's POLR2A (RPB1) subunits are highly-conserved proteins that display an overall similar structure even though some minor local differences because of subunit-specific sequences are anticipated.[11] Extrapolating the yeast Pol II structure (PDB 1WCM) onto POLR3A (RPC1), we expect the p.Gln1336X mutation in human POLR3A to be located on the clamp region of Pol III, which corresponds to Glu1417 in POLR2A (RPB1). This mutation is located in an area where the specific subunits POLR3C/POLR3F (RPC62/RPC39) and POLR3G (RPC32) have been localized by immunolabeling and electron microscopy.[12,13] The effect of this mutation is probably drastic and most likely corresponds to an important alteration of the interaction of the ternary POLR3G/POLR3C/POLR3F (RPC32/RPC62/RPC39) complex and/or of the POLR3H/CRCP (RPC8/9) complex (analogous to POLR2D/POLR2G or RPB4/7) with the remainder of the polymerase. The p.Met852Val and p.Cys724Ile mutations in *POLR3A* correspond to the residues Met818 and Val690 in POLR2A (RPB1). The p.Met852Val mutation is located in the cleft region of the polymerase on the bridge helix where incoming double-stranded DNA lies during transcription. The p.Cys724Ile mutation is located in the external 2 region. The p.Asp372Asn (Asp356) and p.Gly672Glu (Gly638) mutations are located in the lobe and the so-called external 1 regions, respectively, that are positioned close by the AC19 subunit of Pol III, which is related to the POLR2J (RPB11) subunit of Pol II. The p.Asn775Ile mutation in POLR3A corresponds to Asn741 in POLR2A, which is located in the external 1 region of Pol II. The p.Phe558Leu, p.Ser636Tyr, and p.Arg1005Cys mutations in POLR3A correspond to Phe540, Asn603, and Arg1036 residues in POLR2A and are located at the end of the fork region, the external 2, and the hybrid binding areas of POLR2A (RPB1), respectively. They are all located in the vicinity of POLR2H (RPB8) (a shared subunit between Pol I, Pol II, and Pol III). These mutations might alter the local environment, leading to modified interaction of the polymerase with its RPB8 subunit.

The three nonsense mutations and the two splice-site mutations were predicted to lead to truncated proteins of different sizes (Figure 1). The six individuals from the large Syrian LO family X are homozygote for an intronic variant c.2003+18G>A (p.Tyr637CysfsX650), whereas two individuals with 4H from families V and VIII share the same c.2711-1G>A (p.Arg873AlafsX878) intronic variant. The mutational impact of these two variants was assessed with Splice View and Slice Port. The Syrian G to A substitution at position c.2003+18 was predicted to create a new donor splice site, and this was confirmed by RT-PCR and sequencing of the PCR products. This mutation causes the retention of 19 nucleotides from intron 14 leading to an addition of six amino acids to the protein, changing

the reading frame and a premature stop codon at position 650. RT-PCR amplification revealed that both the normal and the aberrantly spliced products are produced, suggesting that some normal *POLR3A* is still expressed (Figure S1, available online). The mutation c.2711-1G>A is predicted to remove an acceptor site; lead to the use of a cryptic acceptor site located in exon 20, five base pairs past the original site; and cause a change in the reading frame and a premature stop codon at position 878.

The role of Pol III as a housekeeping gene might explain the absence of individuals with two null alleles. The nature of the uncovered mutations suggests a rather hypomorphic dysfunction of Pol III because of a decreased abundance of POLR3A or abnormal interactions of POLR3A with DNA, other Pol III subunits, or transcription factors. We performed immunoblots by using the previously validated hRPC155 antibody[14] in whole-cell lysates derived from the fibroblasts of four individuals with 4H to assess whether POLR3A levels are indeed reduced (Figures 2A and 2B). The relative ratio of POLR3A, which is normalized to actin in fibroblasts, from affected individuals is significantly lower (23.4%) than in controls (Figure 2B). The relative ratio of the four individuals with 4H versus the two controls is also reduced, and this was shown to be statistically significant (p = 0.001) (Figure 2C). These results suggest that regardless of the nature of the mutations, POLR3A is less abundant in fibroblasts from affected individuals. To establish whether POLR3A was also reduced in the central nervous system, we performed an immunoblot on protein extracts from the brain of individual 9, who was diagnosed with 4H and was a carrier of one missense mutation and one nonsense mutation, and we compared this immunoblot to that of an age-matched control (Figure 2D). Figure 2E shows a significant reduction in POLR3A levels in the cortex and cerebral white matter. The most significant decrease was observed in the white matter of those with 4H (26.8%, p = 0.006) compared to the white matter of the control (Figure 2E).

POLR3A mutations cause three overlapping leukodystrophy phenotypes (Table 1). These individuals all have in common progressive upper motor neuron dysfunction as well as some degree of cerebellar involvement and cognitive regression. Mean age of loss of ambulation in this cohort is 16.1 years. They also all demonstrate a hypomyelinating pattern on MRI; there is isointense or only minimally hypointense white matter in T1-weighted images and hyperintense white matter in T2-weighted images.[15] The deep white matter is preferentially involved, and of the U-fibers are relatively spared (Figure 3). Less constant MRI findings include a thin corpus callosum and preferential vermian cerebellar atrophy. Despite their clinical and radiological similarities, TACH, LO, and 4H have some distinct features suggesting that Pol III-related leukodystrophies correspond to a spectrum with inter- and intrafamilial variability. Individuals with TACH have the earliest age of onset and are more likely to present in childhood with developmental delays. In our cohort, indi-

viduals with TACH required a wheelchair for daily use earlier than individuals with 4H or LO, at a mean age of 8.25 years, though two individuals are still ambulatory at ages 14 and 19. The severity of the disease is highly variable in individuals with TACH homozygote for the same c.2015G>A mutation, even in the same family. Eye-movement abnormalities such as an abnormal smooth pursuit and vertical gaze limitations were seen more commonly in TACH and 4H syndrome than in LO. Although optic atrophy was a frequent feature in TACH (four out of six individuals), it was not seen in LO and 4H. Peripheral-nerve involvement is also not a constant finding. Nerve biopsies were performed in three of the five individuals with 4H and showed the typical abnormalities described in this disorder visible by electron microscopy: clefts lined with granular debris, expanded abaxonal space, outpocketing with vacuolar disruption, and loss of normal myelin periodicity.[8] Nerve biopsies performed on two individuals with TACH and one individual with LO were completely normal. Although hypodontia was present in all individuals with 4H or LO in this cohort, it was only observed in two out of six individuals with TACH. Hypogonadotropic hypogonadism was by definition seen in all individuals with 4H but was found in only two out of six individuals with TACH and none of the individuals with LO. However, the young age of some of the individuals with LO and TACH might have prevented a diagnosis of hypogonadotropic hypogonadism. Therefore, hypodontia and hypogonadotropic hypogonadism are not universally found in Pol III-related leukodystrophies but when present should encourage clinicians to search for *POLR3A* mutations. Only the identification of a greater number of *POLR3A*-mutation-proven cases of hypomyelinating leukodystrophy will allow a better definition of the full clinical spectrum and a genotype-phenotype correlation.

Only recently, the first human mutations in POLR1D, a shared subunit of Pol I and Pol III, were found to cause a dominant developmental disease with no central nervous disease involvement: Treacher Collins syndrome (TCS [MIM 154500]).[16] The uncovering of recessive mutations in other individuals with TCS in the gene encoding the Pol I subunit POLR1C closely interacting with POLR1D suggests that Pol I rather than Pol III dysregulation is more central to TCS's pathophysiology. Nuclei of human cells contain three DNA dependent RNA polymerases (Pol I, Pol II, and Pol III) that are each responsible for the transcription of specific sets of genes.[17] Pol I transcribes the large ribosomal RNA that is subsequently processed into 28S, 18S, and 5.8S RNAs, which represent major constituents of the ribosome.[18] Pol II transcribes all protein coding messenger RNA (mRNA), most small nuclear RNAs (snRNAs), small nucleolar RNAs, and probably all microRNAs (miRNAs).[18] Pol III is involved in the transcription of small RNAs that do not code for proteins but that are essential for the regulated execution of gene expression programs. These Pol III transcribed RNAs include transfer RNAs (tRNAs), the ribosomal 5S RNA, U6 snRNA, and

**Table 1. Mutations and Clinical Features of Pol III-Related Leukodystrophies**

Individual Number	Family Number	Ethnicity	Diagnosis	DNA	Protein	Gender	Age of Onset (Years)	Developmental Delay	Cognitive Regression	Seizures	Optic Atrophy	Gaze-Evoked Nystagmus	Abnormal Smooth Pursuits	Vertical Gaze Limitation	Dysphagia	Hypersalivation	Upper motor Neuron Signs	Tremor	Cerebellar Signs	Wheelchair	Age of Wheelchair Use (Years)	Hypodontia	Hypogonadotropic Hypogonadism	Nerve Biopsy	Age of Death
1	I	FC	TACH	c.1674C>G / c.3742insACC	p.Phe558Leu / p.1248insThr	M	2	+	+	– –	–	+	+	–	–		+	+	+	+	5	–	–	N/A	–
2	II	FC	TACH	c.2015G>A	p.Gly672Glu	M	1	+	+	+	+	+	+	+	+	+	+	+	+	+	8	+	–	N/A	–
3	II	FC	TACH	c.2015G>A	p.Gly672Glu	M	5	+	+	–	–	+	–	–	–	+	+	+	–	–		+	–	N/A	–
4	II	FC	TACH	c.2015G>A[a]	p.Gly672Glu[a]	F	3	–	+	+	–	+	–	–	+	+	+	+	+	+	8	–	–	–	21
5	III	FC	TACH	c.2015G>A	p.Gly672Glu	M	3	–	+	–	–	+	+	+	+	+	+	+	+	+	12	–	+	–	–
6	IV	FC	TACH	c.2015G>A	p.Gly672Glu	F	5	–	+	–	+	–	+	–	+	–	+	–	–	–		–	+	N/A	–
7	V	W USA	4H	c.2554A>G / c.2711-1G>A	p.Met852Val / p.Arg873AlafsX878	F	13	–	+	±	–	–	+	+	+	+	+	–	+	+	24	+	+	+	–
8	VI	AA USA	4H	c.2324A>T / c.1114G>A	p.Asn775Ile / p.Asp372Asn	F	0	+	+	–	–	+	+	+	+	+	–	+	+	10	+	+	N/A	–
9	VII	W USA	4H	c.2830G>T / c.3013C>T	p.Glu944X / p.Arg1005Cys	M	13	–	+	±	–	–	+	+	+	–	+	–	+	+	30	+	+	+	36
10	VIII	W USA	4H	c.2554A>G / c.2711-1G>A	p.Met852Val / p.Arg873AlafsX878	F	12	–	+	–	–	–	+	+	+	+	+	–	+	+	24	+	+	+	–
11	IX	France	4H	c.4006C>T / c.1907C>A	p.Gln1336X / p.Ser636Tyr	F	1	+	+	–	–	+	–	–	+	+	+	–	–	–		+	+	N/A	–
12	X	Syria	LO	c.2003+18G>A	p.Tyr637CysfsX650	M	13	–	+	–	–	–	–	–	–	+	+	+	+	23	+	–	N/A	28
13	X	Syria	LO	c.2003+18G>A	p.Tyr637CysfsX650	F	12	–	+	–	–	–	–	–	–	+	+	+	+	20	+	–	N/A	–
14	X	Syria	LO	c.2003+18G>A	p.Tyr637CysfsX650	F	11	–	+	–	–	–	–	–	–	+	+	+	+	20	+	–	N/A	–

Table 1. Continued

Individual Number	Family Number	Ethnicity	Diagnosis	DNA	Protein	Gender	Age of Onset (Years)	Developmental Delay	Cognitive Regression	Seizures	Optic Atrophy	Gaze-Evoked Nystagmus	Abnormal Smooth Pursuits	Vertical Gaze Limitation	Dysphagia	Hypersalivation	Upper motor Neuron Signs	Tremor	Cerebellar Signs	Wheelchair	Age of Wheelchair Use (Years)	Hypodontia	Hypogonadotropic Hypogonadism	Nerve Biopsy	Age of Death
15	X	Syria	LO	c.2003+18G>A	p.Tyr637CysfsX650	F	11	−	+	−	−	−	−	−	−	−	+	−	+	−	−	+	−	N/A	−
16	X	Syria	LO	c.2003+18G>A	p.Tyr637CysfsX650	M	12	−	+	−	−	−	−	−	−	−	+	−	+	−	−	+	−	N/A	−
17	X	Syria	LO	c.2003+18G>A	p.Tyr637CysfsX650	M	12	−	+	−	−	−	−	−	−	−	+	−	+	−	−	+	−	N/A	−
18	XI	W Europe	LO	c.418C>T / c.2554A>G	p.Arg140X / p.Met852Val	F	3	+	+	−	−	−	+	−	−	−	+	+	+	−	−	+	−	−	−
19	XII	Guatemala	LO	c.2171G>A	p.Cys724Tyr	M	2	+	+	−	−	−	+	+	−	+	+	+	+	+	9	+	N/A	N/A	−

POLR3A mutations and clinical features of individuals with TACH, 4H, and LO. A total of 14 different mutations were found: missense, nonsense, insertion, and splice-site mutations. Individuals 1-5[3] and 6[10] with TACH, individuals 7-10[8] with 4H and individuals 12-17[4,5] with LO have been published previously. The following abbreviations are used: +, positive or present; −, negative or absent; FC, French-Canadian; AA USA, African American from USA; W Europe, white from Europe; W USA, white from USA; F, female; M, male; and N/A, not available.

a Presumed mutation the deceased individual 4 for which DNA was not available.
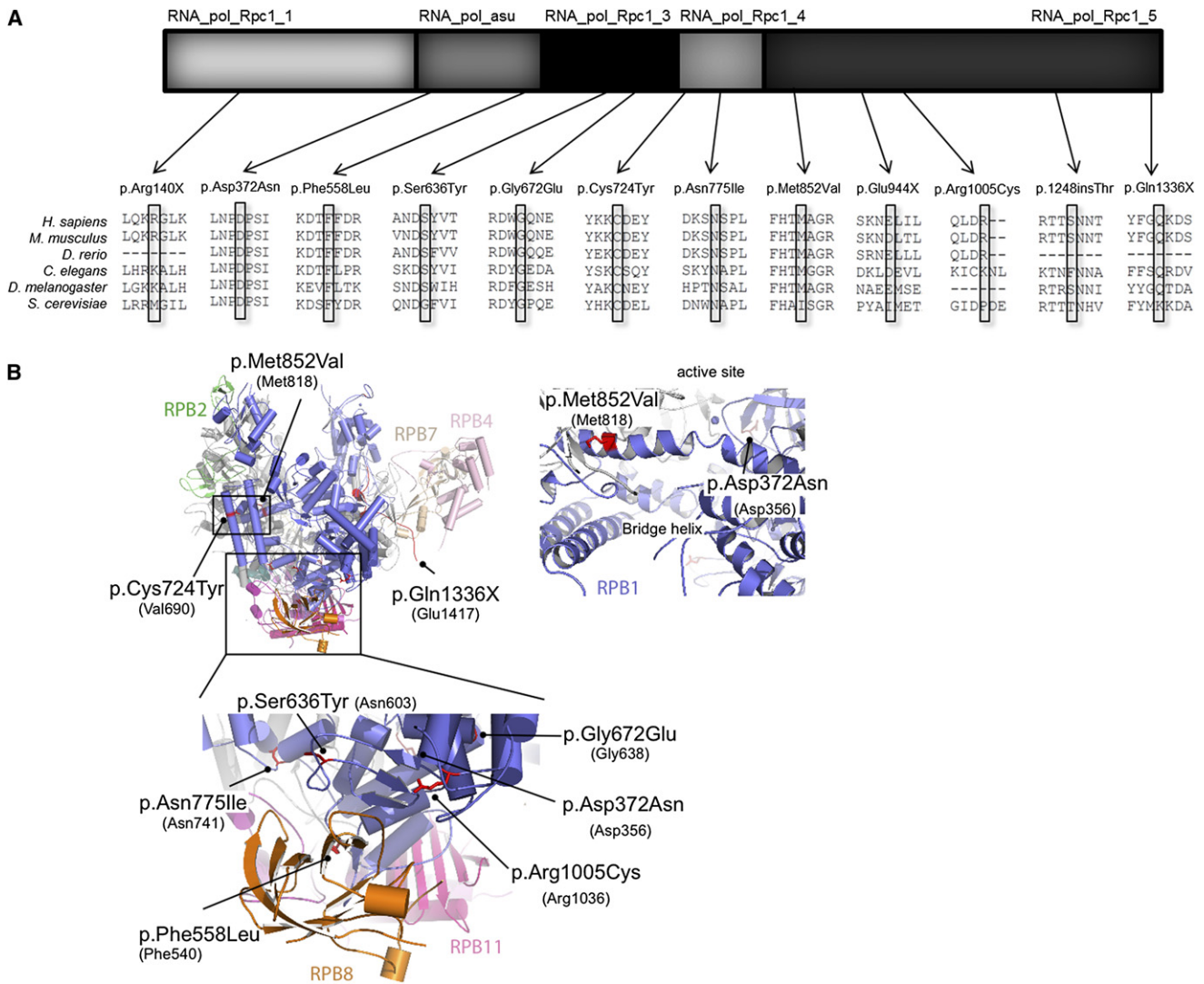
Figure 1. POLR3A Mutations

(A) Schematic representation of POLR3A exonic mutations. Missense and nonsense mutations are depicted according to the different POLR3A (RPC1) domains (modified from Ensembl). The amino acid conservation across species is shown for all missense and nonsense mutations. The following abbreviations are used in the upper panel: RNA_pol_Rpc1_1, RNA_pol_Rpc1_3, RNA_pol_Rpc1_4, and RNA_pol_Rpc1_5, RNA polymerase subunit domains one, three, four and five; and RNA_pol_asu, RNA polymerase alpha subunit. The following abbreviations are used in the lower panel: *C. elegans*, *Caenorhabditis elegans*; *D. melanogaster*, *Drosophila melanogaster*; *D. rerio*, *Danio rerio*; *H. sapiens*, *Homo sapiens*; *M. musculus*, *Mus musculus*; and *S. cerevisiae*, *Saccharomyces cerevisiae*.

(B)Three-dimensional representations of POLR3A missense and nonsense mutations. Point mutations identified in POLR3A are displayed according to their equivalent positions in the yeast RNA Polymerase II RPB1 subunit.[27] Numbers in brackets refer to the positions in yeast RPB1. Images have been generated with PyMol software (Schrödinger). For imaging purposes, the RPB5 subunit has been omitted from the figure. RPB1 is shown in blue, RPB2 in green, RPB7 in brown, RPB4 in pink, RPB8 in orange, and RPB11 in magenta.

7SK RNA, as well as small interspersed repetitive sequences (SINEs).[17,19,20] Pol III's transcription is cell-type and cell-cycle dependent[20] and is dysregulated during cellular transformation.[17,21] RNA polymerases are multisubunit complexes that are composed of 12 (Pol II), 14 (Pol I), or 17 (Pol III) subunits. They are highly-conserved and important homologies have been found between the three Pols. *POLR3A* encodes the largest subunit of Pol III, which, together with POLR3B, constitutes the RNA catalytic site of Pol III.[22] POLR3A interacts with multiple subunits of Pol III, including subunits that are common to all three RNA polymerases (POLR2E, POLR2F, POLR2H, and

POLR2K) and two that are shared by Pol I and Pol III only (POLR1C and POLR1D).[12] In addition, POLR3A interacts with subunits specific to Pol III, most notably POLR3G that forms a ternary subcomplex with POLR3C and POLR3F, which is positioned between POLR3A and its transcription initiation factors.[17,22]

Considering that Pol III is central to tRNA production, it is tempting to hypothesize that *POLR3A* mutations lead to dysregulation of Pol III, which could influence relative levels of certain tRNA that are known to be more abundant in the central nervous system.[23] Two other leukoencephalopathies are caused by mutations in genes
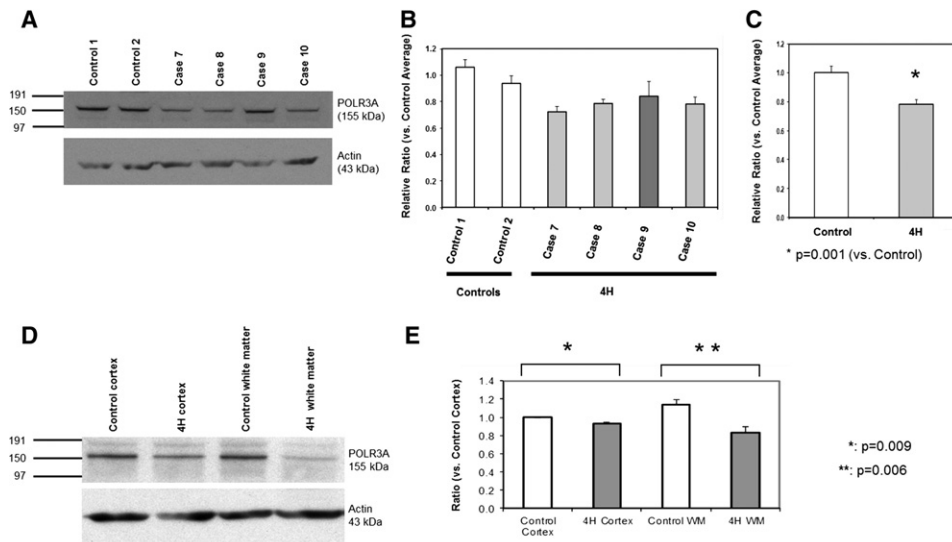
Figure 2. Immunoblots of Fibroblasts and Brain Lysates from Individuals with 4H and from Controls
(A) POLR3A immunoblot of 4H fibroblasts versus controls. Cultured fibroblasts were lysed with RIPA buffer. Protein samples were electrophoresed with SDS-PAGE and blotted onto nitrocellulose membranes. Immunoblots were imaged with QuantityOne software (BioRad) and the density of each was quantified across triplicate experiments and averaged with normalization to a loading control (actin). A typical image of POLR3A immunoblot done on 4H and control fibroblasts with anti-hRPC155 at 1:2000 dilution.[14] From left to right, samples are control 1 and 2 and individuals 7, 8, 9, and 10.
(B) Ratio of POLR3A in 4H fibroblasts versus in control fibroblasts. Actin was used as a loading control. Controls are shown in white, and individuals with 4H are shown in gray. Standard error calculation is reported for repeated experiments.
(C) Ratio of POLR3A in 4H fibroblasts versus two control fibroblasts showing 21.67% decrease of POLR3A in 4H fibroblasts (p = 0.001). The average of two controls is shown in white, and the average of the individuals with 4H is shown in gray. Standard error calculation is reported for repeated experiments. Statistical analysis was carried out with a student t test.
(D) Immunoblot of the brain of individual 9 compared to the brain of a control. Typical image of a POLR3A immunoblot done on the cortex and white matter of individual 9, diagnosed with 4H, and an age-matched control with anti-hRPC155 at 1:2000 dilution. The control is shown in white, and the individual with 4H is shown in gray. From left to right, samples are a control cortex, a 4H cortex, control white matter, and 4H white matter.
(E) Relative ratio of POLR3A in the brain of individual 9, affected by 4H syndrome versus that in a control; there is a 6.8% decrease of POLR3A in the 4H cortex compared to a control (p = 0.009) and a 26.8% decrease of POLR3A in 4H white matter compared to that in a control (p = 0.006). Standard error calculation is reported for repeated experiments. Statistical analysis was carried out with a student t test.

important for protein synthesis: leukoencephalopathy with spinal cord involvement and lactate elevation (LBSL [MIM 611105]) caused by mutations in the nuclear-coded mitochondrial aspartyl-tRNA synthetase (*DARS2* [MIM 610956]) and hypomyelinating leukodystrophy-3 (MIM 260600) caused by mutation in aminoacyl-tRNA synthetase complex-interacting multifunctional protein 1 (*AIMP1/p43* [MIM 603605]) important for proper cytoplasmic protein synthesis.[24–26] Pol III-related leukodystrophies and these other leukoencephalopathies could reflect the vulnerability of the central nervous system to adequate expression of certain tRNAs during development.

Supplemental Data

Supplemental Data include one figure and one table and can be found with this article online at http://www.cell.com/AJHG/.

Acknowledgments

Figure 3. MRI Findings in 4H Subject 9
(A) Axial T2-weighted image of the brain at the level of the pons.
(B) Axial T2-weighted image of the brain at the level of the basal ganglia.
(C) Sagittal T1-weighted image of the brain at the midline.
(D) Axial T1-weighted image of the brain at the level of the pons.
(E) Axial T1-weighted image of the brain at the level of the basal ganglia.
As previously described,[15] this case demonstrates the features characteristic of 4H visible through neuroimaging: cerebellar white matter mild T2 hyperintensity with relative T2 darkness of the dentate nucleus (A, small white arrow); T2 hypointensity of the optic radiations and lateral nucleus of the thalamus (B, small black arrows); cerebellar atrophy (C, large white arrow); and T1 isointensity to hyperintensity of the white matter (D and E), consistent with a radiologic diagnosis of hypomyelination.

Web Resources

The URLs for data presented herein are as follows:

Ensembl, http://www.ensembl.org/index.html
Online Mendelian Inheritance in Man (OMIM), http://www.omim.org
Splice View, http://zeus2.itb.cnr.it/~webgene/wwwspliceview_ex.html
Human Splicing Finder, http://www.umd.be/HSF/

References

1. Schiffmann, R., and van der Knaap, M.S. (2004). The latest on leukodystrophies. Curr. Opin. Neurol. *17*, 187–192.
2. Schiffmann, R., and van der Knaap, M.S. (2009). Invited article: An MRI-based approach to the diagnosis of white matter disorders. Neurology *72*, 750–759.
3. Bernard, G., Thiffault, I., Tetreault, M., Putorti, M.L., Bouchard, I., Sylvain, M., Melançon, S., Laframboise, R., Langevin, P., Bouchard, J.P., et al. (2010). Tremor-ataxia with central hypomyelination (TACH) leukodystrophy maps to chromosome 10q22.3-10q23.31. Neurogenetics *11*, 457–464.
4. Atrouni, S., Darazé, A., Tamraz, J., Cassia, A., Caillaud, C., and Mégarbané, A. (2003). Leukodystrophy associated with oligodontia in a large inbred family: Fortuitous association or new entity? Am. J. Med. Genet. A. *118A*, 76–81.
5. Chouery, E., Delague, V., Jalkh, N., Salem, N., Kfoury, J., Rodriguez, D., Chabrol, B., Boespflug-Tanguy, O., Lévy, N., Serre, J.L., and Mégarbané, A. (2011). A whole-genome scan in a large family with leukodystrophy and oligodontia reveals linkage to 10q22. Neurogenetics *12*, 73–78.
6. Wolf, N.I., Harting, I., Innes, A.M., Patzer, S., Zeitler, P., Schneider, A., Wolff, A., Baier, K., Zschocke, J., Ebinger, F., et al. (2007). Ataxia, delayed dentition and hypomyelination: A novel leukoencephalopathy. Neuropediatrics *38*, 64–70.
7. Bekiesinska-Figatowska, M., Mierzewska, H., Kuczynska-Zardzewialy, A., Szczepanik, E., and Obersztyn, E. (2010). Hypomyelination, hypogonadotropic hypogonadism, hypodontia - First Polish patient. Brain Dev. *32*, 574–578.
8. Timmons, M., Tsokos, M., Asab, M.A., Seminara, S.B., Zirzow, G.C., Kaneski, C.R., Heiss, J.D., van der Knaap, M.S., Vanier, M.T., Schiffmann, R., and Wong, K. (2006). Peripheral and central hypomyelination with hypogonadotropic hypogonadism and hypodontia. Neurology *67*, 2066–2069.
9. Vázquez-López, M., Ruiz-Martín, Y., de Castro-Castro, P., Garzo-Fernández, C., Martín-del Valle, F., and Márquez-de la Plata, L. (2008). Central hypomyelination, hypogonadotrophic hypogonadism and hypodontia: A new leukodystrophy. Rev. Neurol. *47*, 204–208.
10. Tetreault, M., Putorti, M.L., Thiffault, I., Sylvain, M., Vanderver, A., Schiffmann, R., Brais, B., and Bernard, G. (2011). Refinement of the locus responsible for Tremor-Ataxia with Central Hypomyelination (TACH) leukodystrophy to chromosome 10q22.3-23.1. Can. J. Neurol. Sci., in press.
11. Jasiak, A.J., Armache, K.J., Martens, B., Jansen, R.P., and Cramer, P. (2006). Structural biology of RNA polymerase III: Subcomplex C17/25 X-ray structure and 11 subunit enzyme model. Mol. Cell *23*, 71–81.
12. Fernández-Tornero, C., Böttcher, B., Riva, M., Carles, C., Steuerwald, U., Ruigrok, R.W., Sentenac, A., Müller, C.W., and Schoehn, G. (2007). Insights into transcription initiation and termination from the electron microscopy structure of yeast RNA polymerase III. Mol. Cell *25*, 813–823.
13. Werner, M., Hermann-Le Denmat, S., Treich, I., Sentenac, A., and Thuriaux, P. (1992). Effect of mutations in a zinc-binding domain of yeast RNA polymerase C (III) on enzyme function and subunit association. Mol. Cell. Biol. *12*, 1087–1095.
14. Sepehri, S., and Hernandez, N. (1997). The largest subunit of human RNA polymerase III is closely related to the largest subunit of yeast and trypanosome RNA polymerase III. Genome Res. *7*, 1006–1019.

15. Steenweg, M.E., Vanderver, A., Blaser, S., Bizzi, A., de Koning, T.J., Mancini, G.M., van Wieringen, W.N., Barkhof, F., Wolf, N.I., and van der Knaap, M.S. (2010). Magnetic resonance imaging pattern recognition in hypomyelinating disorders. Brain *133*, 2971–2982.

16. Dauwerse, J.G., Dixon, J., Seland, S., Ruivenkamp, C.A., van Haeringen, A., Hoefsloot, L.H., Peters, D.J., Boers, A.C., Daumer-Haas, C., Maiwald, R., et al. (2011). Mutations in genes encoding subunits of RNA polymerases I and III cause Treacher Collins syndrome. Nat. Genet. *43*, 20–22.

17. Dumay-Odelot, H., Durrieu-Gaillard, S., Da Silva, D., Roeder, R.G., and Teichmann, M. (2010). Cell growth- and differentiation-dependent regulation of RNA polymerase III transcription. Cell Cycle *9*, 3687–3699.

18. Cramer, P., Armache, K.J., Baumli, S., Benkert, S., Brueckner, F., Buchen, C., Damsma, G.E., Dengl, S., Geiger, S.R., Jasiak, A.J., et al. (2008). Structure of eukaryotic RNA polymerases. Annu. Rev. Biophys. *37*, 337–352.

19. Dieci, G., Fiorino, G., Castelnuovo, M., Teichmann, M., and Pagano, A. (2007). The expanding RNA polymerase III transcriptome. Trends Genet. *23*, 614–622.

20. Haurie, V., Durrieu-Gaillard, S., Dumay-Odelot, H., Da Silva, D., Rey, C., Prochazkova, M., Roeder, R.G., Besser, D., and Teichmann, M. (2010). Two isoforms of human RNA polymerase III with specific functions in cell growth and transformation. Proc. Natl. Acad. Sci. USA *107*, 4176–4181.

21. White, R.J. (2011). Transcription by RNA polymerase III: More complex than we thought. Nat. Rev. Genet. *12*, 459–463.

22. Werner, M., Thuriaux, P., and Soutourina, J. (2009). Structure-function analysis of RNA polymerases I and III. Curr. Opin. Struct. Biol. *19*, 740–745.

23. Dittmar, K.A., Goodenbour, J.M., and Pan, T. (2006). Tissue-specific differences in human transfer RNA expression. PLoS Genet. *2*, e221.

24. Feinstein, M., Markus, B., Noyman, I., Shalev, H., Flusser, H., Shelef, I., Liani-Leibson, K., Shorer, Z., Cohen, I., Khateeb, S., et al. (2010). Pelizaeus-Merzbacher-like disease caused by AIMP1/p43 homozygous mutation. Am. J. Hum. Genet. *87*, 820–828.

25. Scheper, G.C., van der Klok, T., van Andel, R.J., van Berkel, C.G., Sissler, M., Smet, J., Muravina, T.I., Serkov, S.V., Uziel, G., Bugiani, M., et al. (2007). Mitochondrial aspartyl-tRNA synthetase deficiency causes leukoencephalopathy with brain stem and spinal cord involvement and lactate elevation. Nat. Genet. *39*, 534–539.

26. Boespflug-Tanguy, O., Aubourg, P., Dorboz, I., Bégou, M., Giraud, G., Sarret, C., and Vaurs-Barrière, C. (2011). Neurodegenerative disorder related to AIMP1/p43 mutation is not a PMLD. Am. J. Hum. Genet. *88*, 392–393, author reply 393–395.

27. Armache, K.J., Mitterweger, S., Meinhart, A., and Cramer, P. (2005). Structures of complete RNA polymerase II and its subcomplex, Rpb4/7. J. Biol. Chem. *280*, 7131–7134.